Temperature dependence of current self-oscillations and electric-field domains in sequential-tunneling doped superlattices

David Sánchez,[1] L. L. Bonilla,[2,3] and G. Platero[1]
[1]*Instituto de Ciencia de Materiales de Madrid (CSIC), Cantoblanco, 28049 Madrid, Spain*
[2]*Departamento de Matemáticas, Escuela Politécnica Superior, Universidad Carlos III de Madrid, Avenida de la Universidad 30, 28911 Leganés, Spain*
[3]*Unidad Asociada al Instituto de Ciencia de Materiales de Madrid (CSIC), Madrid, Spain*
(Received 6 April 2001; published 28 August 2001)

We examine how the current-voltage characteristics of a doped weakly coupled superlattice depends on temperature. The drift velocity of a discrete drift model of sequential tunneling in a doped GaAs/AlAs superlattice is calculated as a function of temperature. Numerical simulations and theoretical arguments show that increasing temperature favors the appearance of current self-oscillations at the expense of static electric-field domain formation. Our findings agree with available experimental evidence.

DOI: 10.1103/PhysRevB.64.115311 PACS number(s): 73.40.−c, 72.20.Ht

I. INTRODUCTION

Manifestations of vertical transport in weakly coupled semiconductor-doped superlattices (SL's) include electric-field domain formation,[1–3] multistability,[4–6] self-sustained current oscillations,[7–9] and driven and undriven chaos.[10] Stationary electric-field domains appear in voltage-biased SL's if the doping is large enough.[11] When the carrier density is below a critical value, self-sustained oscillations of the current may appear. They are due to the dynamics of the domain wall separating the electric-field domains. This domain wall moves through the structure and is periodically recycled. The frequencies of the corresponding oscillation depend on the applied bias and range from the kHz to the GHz regime. Self-oscillations persist even at room temperature, which makes these devices promising candidates for microwave generation.[7] Numerical calculation of the voltage-doping SL phase diagram shows that only static electric-field domains are possible for high enough SL doping. As the doping decreases, voltage windows where current self-oscillations are possible open up.[12] These windows may coalesce into a single one as doping is further lowered and oscillations disappear below a critical doping value. Since doping is not a feasible control parameter, other quantities affecting carrier density should be used to observe these behaviors. Feasible control parameters are laser illumination in undoped SL's (Refs. 13–15) (which behaves qualitatively as well doping), transverse magnetic fields,[16] and temperature[7,14,17–19] in doped SL's.

Despite its practical and theoretical interest, the effect of temperature on electric-field domains[20–22] and current self-oscillations is still poorly understood. Early numerical calculations were performed with a fixed drift velocity corresponding to a fixed temperature.[7] Using the insight provided by these calculations and reasonable expectations on how drift velocity depends with temperature, the fact that oscillatory voltage windows widen as the temperature increases was explained.[14] More detailed experimental studies dealing with the influence of temperature on self-oscillations have appeared recently.[17–19] Experimental data show that raising the temperature is similar to lowering the SL doping. At low temperature a multiplicity of purely static states (corresponding to the coexistence of low- and high-field domains in the SL) was observed. As the temperature increased, voltage windows corresponding to self-oscillations appeared and widened in the SL I-V characteristics.[18] Experimental data were interpreted by using the discrete drift model[13] with a fitted drift velocity.[19] These authors concluded that the peak-to-valley ratio in the negative differential mobility region of the drift velocity was crucial to understand the data. A model including both variation of the electron density in the wells and variation of the drift velocity with temperature was therefore needed.[19]

In a recent paper, we have been able to derive discrete drift-diffusion (DDD) models, including boundary conditions, from microscopic sequential-tunneling models.[23] By using our formulas for the field-dependent drift velocity at different temperatures (ranging from 0 to 175 K), we can compare numerical simulations of these simple discrete models with the experimental data of Wang *et al*. Our results show that increasing temperature facilitates current self-oscillations in the second plateau. Furthermore, our numerical results (based upon microscopically calculated drift velocities) agree with the available experimental data and explain them quantitatively. We explain qualitatively why regions of stationary states alternate with regions of self-oscillations in the temperature-voltage phase diagram. Finally and on the basis of our numerical simulations, we also explain why the frequency may have local maxima in the voltage intervals where self-oscillations occur. That the frequency may increase with voltage, while the average current simultaneously decreases, is thus a consequence of our theory, not an anomaly.[17,18]

The rest of this paper is as follows. Section II contains a brief description of the DDD model and a calculation of its transport coefficients and boundary conditions appropriate for the experimental sample of Wang *et al*. Results of numerical simulations of this model and comparison with experimental data are reported in Sec. III. Section IV contains our conclusions. A discussion of the qualitative theoretical

analysis included in the experimental papers is presented in the Appendix.

II. DISCRETE DRIFT-DIFFUSION MODEL

The main charge transport mechanism in a weakly coupled SL is sequential resonant tunneling. The characteristics of the samples experimentally studied in Ref. 18 are such that the macroscopic time scale of the self-sustained oscillations is larger than the tunneling time (defined as the time an electron needs to advance from one well to the next one). In turn, this latter time is much larger than the intersubband scattering time. Then tunneling across a barrier is a stationary process with well-defined Fermi-Dirac distributions at each well. These distributions depend on the instantaneous values of the electron density and potential drops and vary only on the longer macroscopic time scale. The tunneling current density across each barrier in the SL may be approximately calculated by means of the transfer Hamiltonian method.[5] The resulting formulas can be used to calculate the transport coefficients and boundary conditions of the following DDD model:[23]

$$\frac{\varepsilon}{e}\frac{dF_i}{dt}+\frac{n_i v(F_i)}{\mathcal{L}}-D(F_i)\frac{n_{i+1}-n_i}{\mathcal{L}^2}=J(t), \tag{1}$$

$$F_i-F_{i-1}=\frac{e}{\varepsilon}(n_i-N_D^w). \tag{2}$$

In these equations, ε, e, and N_D^w are well permittivity, minus the electron charge and two-dimensional (2D) doping in the wells, respectively. $\mathcal{L}=d+w$ is the SL period, where d and w are the widths of barriers and wells, respectively. Equation (1) is Ampère's law establishing that the total current density eJ is the sum of displacement and tunneling currents. The latter consists of a drift term $en_i v(F_i)/\mathcal{L}$ and a diffusion term, $eD(F_i)(n_{i+1}-n_i)/\mathcal{L}^2$.[24] We have adopted the convention (usual in this field) that the current density has the same direction as the flow of electrons. Equation (1) holds for $i=1,\ldots,N-1$. Equation (2) is the Poisson equation, and it holds for $i=1,\ldots,N$. Here n_i is the 2D electron number density at well i, which is singularly concentrated on a plane located at the end of the well. F_i is *minus* an average electric field on a SL period comprising the ith well and the ith barrier (well i lies between barriers $i-1$ and i: barriers 0 and N separate the SL from the emitter and collector contact regions, respectively).

Figure 1 depicts the field-dependent drift velocity at different temperatures for SL parameter values of Ref. 17: 40 periods of 14 nm GaAs and 4 nm AlAs and well doping $N_D^w=2\times10^{11}$ cm^{-2}. It has been calculated from the microscopic tunneling current density by the procedure explained in Ref. 23. The only adjustable parameter in the sequential tunneling formulas is the Lorentzian half-width of the scattering amplitudes, γ. In a doped SL, the most relevant in-well scattering mechanisms are scattering with ionized impurities (low temperatures) and with LO phonons (high temperatures).[1] To estimate γ we have considered that the voltage difference ΔV between the peaks of two consecutive branches on the second plateau of the static I-V characteristic is

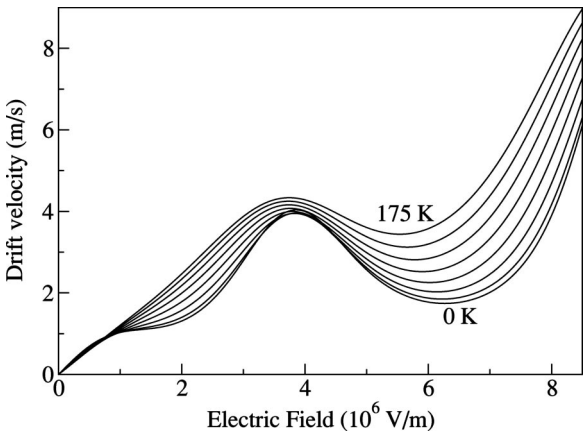

FIG. 1. Drift velocity vs electric field for different temperatures (starting at 0 K up to 175 K in 25 K steps) for a 40-well 14-nm GaAs and 4-nm AlAs SL. Well doping is $N_D^w=2\times10^{11}$ cm^{-2}.

$$\Delta V\approx\epsilon_{C3}-\epsilon_{C2}-2\eta\gamma. \tag{3}$$

Here ϵ_{Ci} is the ith energy level of a given well. For $\gamma=0$, the field profile on the second plateau corresponds to two coexisting electric-field domains with fields $(\epsilon_{C2}-\epsilon_{C1})/[e(d+w)]$ and $(\epsilon_{C3}-\epsilon_{C1})/[e(d+w)]$. The domain walls corresponding to two adjacent branches in the I-V diagram are located in adjacent wells. Then the voltage difference should be $\Delta V\approx\epsilon_{C3}-\epsilon_{C2}$. In the presence of scattering, resonant peaks have finite widths which we take as $2\eta\gamma$, thereby obtaining Eq. (3). Here 2η is an adjustable parameter of the order of unity.[2] By using this formula and the measured current in Ref. 17 (Figs. 2, 3, and 4), we find $\gamma=18$ meV at 1.6 K and $\gamma=23$ meV at 140 K for $\eta\approx0.6$. Linear interpolation yields the temperature dependence of γ in the range we are interested in.

Notice that the first peak of the velocity in Fig. 1 rapidly disappears as the temperature increases for this particular sample. This result might change if we assume different scattering amplitudes for each of the two first subbands of the wells. Moreover, the different extrema of the velocity curve shift to lower field values as the temperature increases. Thus formation of electric-field domains and current self-oscillations are expected for voltages on the second plateau and higher. Multistable solution branches of the current-voltage characteristic curve should also shift to lower voltages and higher currents as the temperature increases, as observed in experiments.[19] These effects could not be obtained from the fitted drift velocity in Ref. 19. As the diffusion coefficient decreases very rapidly with field, we can safely set $D\equiv0$ in our DDD model for the experimentally observed voltage range. The relevant model is thus the well-known discrete drift model of Refs. 13 and 7 with the drift velocity deduced from a microscopic calculation of the current plus boundary conditions[23] (see Fig. 1).

To complete the description of our model, we need to specify initial, boundary, and bias conditions. The dc voltage bias condition is

$$\mathcal{L}\sum_{i=1}^{N} F_i = V. \tag{4}$$

Given that $D(F_i)\equiv 0$, we need only one boundary condition specifying F_0 (the field at the contact region). We will assume that there is an excess electron density in the first well due to tunneling from the highly doped contact region,[7]

$$n_1 = (1+c)N_D^w. \tag{5}$$

For an appropriately chosen dimensionless positive constant c, this condition selects recycling of charge monopole waves as the mechanism for self-sustained oscillations of the current.[7] The same behavior can be obtained from more elaborated boundary conditions for the microscopic tuneling current between the emitter and the neighboring well[23] provided that contact doping is sufficiently high (Ohmic behavior). Given the uncertainties inherent to contact specification, we have preferred to use the phenomenological boundary condition (5) instead.

III. NUMERICAL SIMULATIONS AND COMPARISON WITH EXPERIMENTS

In this section, we shall numerically simulate the discrete drift model for different values of temperature. From formulas (1) and (2), considering $D=0$,

$$\frac{\varepsilon}{e}\frac{dF_i}{dt} + \frac{v(F_i)}{\mathcal{L}}\left[N_D^w + \frac{\varepsilon}{e}(F_i - F_{i-1})\right] = J(t), \tag{6}$$

$$\sum_{i=1}^{N} F_i = \frac{V}{\mathcal{L}}. \tag{7}$$

The corresponding drift curves are chosen among those depicted in Fig. 1 and the boundary condition will be Eq. (5) with $c=10^{-3}$.

A first interesting conclusion can be drawn effortlessly from an analytical upper bound of the critical doping above which there are stable static electric-field domain branches:[11]

$$N_{Dc}^w = \varepsilon v_m \frac{F_m - F_M}{e(v_M - v_m)}. \tag{8}$$

In this formula, F_M and F_m are the values of the electric field which correspond to the maximum and minimum of the drift velocity (v_M and v_m) on the second plateau. The temperature dependence of this critical doping is plotted in Fig. 2. We observe that the critical doping increases with temperature, indicating that the voltage range for which self-oscillations exist increases as temperature does. In particular, Fig. 2 predicts a transition temperature at around 93 K whereas about 140 K is experimentally measured.[17,18] Despite the fact that the bound (8) is only a rough approximation, the agreement is rather good. We shall see below that the agreement improves when complete simulations of the DDD model are carried out.

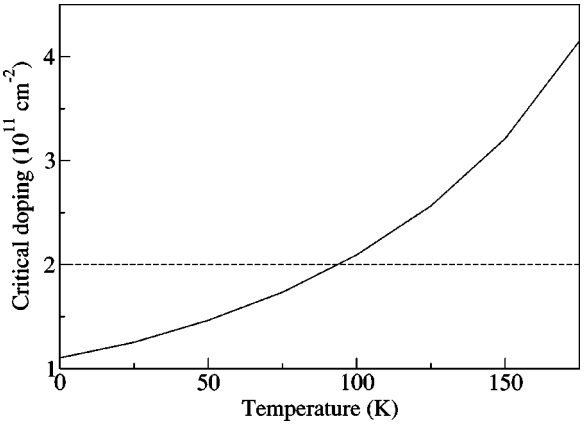

FIG. 2. Bound for the critical doping as a function of temperature (solid line). Experimental value employed in Refs. 17 and 18 (dashed line).

Results of our simulations are presented in Figs. 3 and 4, corresponding to a 40-well SL with $d=4$ nm, $w=14$ nm, $N_D^w = 2\times 10^{11}$ cm^{-2}, and sample area 0.2×0.2 mm^2. Figure 3 shows the time-averaged current-voltage characteristics of such a SL for temperatures ranging from 110 to 150 K. In this temperature range, there are voltage intervals (with a flat form) in which the SL current is stationary, interspersed in voltage intervals of current self-oscillations corresponding to recycling of charge monopoles. This agrees with experimental results reported by Wang *et al.*[17,18] For temperatures lower than 110 K or higher than 250 K, the ranges of self-oscillations disappear. These figures are similar to those reported in the experiments of Li *et al.*[19]

We observe that the *I-V* curve presents intervals in which the average current increases with voltage, followed by in-

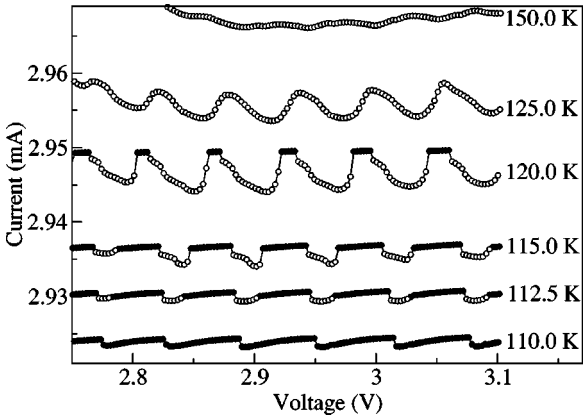

FIG. 3. *I-V* characteristics for different temperatures, showing stationary (dynamic) states with solid (open) circles. The sample is a 40-well 14-nm GaAs and 4-nm AlAs SL. Well doping is $N_D^w = 2\times 10^{11}$ cm^{-2}. Here $c=10^{-3}$ has been used in the numerical simulations. The curve corresponding to 150 K has been shifted -0.04 mA for clarity. Lines are plotted only for eye-guiding purposes.

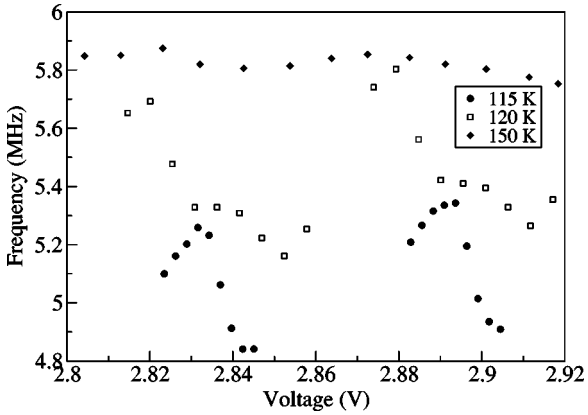

FIG. 4. Current oscillation frequency vs voltage for some dynamic dc bands of the curves shown in Fig. 3.

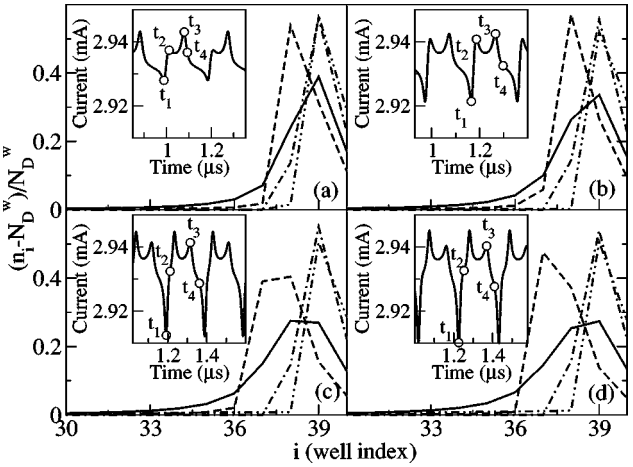

FIG. 5. Nomalized excess of charge at four instants of one period of the current self-oscillations at 115 K. Voltages are (a) 2.824 V, (b) 2.829 V, (c) 2.837 V, and (d) 2.842 V. Real-time current traces are plotted in the insets with the four instants depicted: t_1 (solid lines), t_2 (dashed lines), t_3 (dot-dashed lines), and t_4 (dot-dot-dashed lines).

tervals in which the average current decreases. At lower temperatures the intervals of increasing current are wider whereas the opposite occurs at higher temperatures. Correspondingly, Fig. 4 shows the frequency of the self-oscillations as a function of voltage. The frequency of the self-oscillations in such an interval starts increasing but it drops to a smaller value than the initial one at the upper limit of the interval. The amplitude of the self-oscillations (not shown here) vanishes at the upper and lower limits of each voltage interval. This suggests that the branches of self-oscillations begin and end at supercritical Hopf bifurcations. As the temperature increases, the region of negative differential mobility in Fig. 1 is smoother and the frequency of the self-oscillations increases (see Fig. 4). In the opposite temperature range, at low temperatures, the electric-field profiles consist of basically two stationary domains joined by a domain wall. The *I-V* characteristic curve has multiple branches corresponding to stationary domains with the domain wall located at different wells. This situation resembles that obtained as voltage and doping are varied, provided that the doping and reciprocal of temperature are assimilated. In Ref. 12 the phase diagram doping voltage of a doped SL was calculated. At low doping (high temperature), the electric field inside the SL is almost homogeneous and stationary. Above a critical value, branches of self-oscillations appear. In this region, there are voltage intervals of stationary electric-field profiles separated by intervals of self-oscillations. The latter arise and disappear (typically) as Hopf bifurcations from stationary states. Above a certain doping (low temperature), the intervals of self-oscillations vanish and only stationary states (consisting of two electric field domains separated by a domain wall) remain. Notice in Fig. 4 that there are voltage intervals where the oscillation frequency increases with voltage, while the average current decreases with voltage. This behavior was dubbed *anomalous* by Wang *et al.*,[18] although it is conveniently explained by the discrete drift model equations as shown by our present simulations. A qualitative explanation of this behavior follows.

First of all, it can be observed in the simulations that the maximum current during one oscillation period does not vary too much, while the minimum current drops precipituously with voltage; see the insets in Fig. 5. This rapid drop of the minimum current and the approximate invariance of the maximum current can be understood from an asymptotic analysis:[8] the current approximately follows part of the velocity curve, $eN_D^w v(F)/\mathcal{L}$, during the motion of a monopole. The monopole is created when the current surpasses the maximum value $eN_D^w v_M/\mathcal{L}$. Then the current decreases with time until either the monopole exits at the receiving contact or the minimum value $eN_D^w v_m/\mathcal{L}$ is reached. The first possibility is attained at low voltages, the second one at high voltages. The current oscillation starts with zero amplitude at the lower end of a voltage interval, so that the current does not depart too much from its maximum value. As the voltage increases, the minima of the current at each oscillation period decrease. What about the dependence of frequency with voltage? It can be shown[7] that the oscillation period T_p may be estimated from the following formula:

$$T_p = \frac{\mathcal{L}}{v_{mon}} M - T_f\left(\frac{v_M}{v_{mon}} - 1\right). \tag{9}$$

Here M is such that $N-M$ represents the number of wells traversed by the charge monopole during one oscillation period, v_{mon} is its average velocity, and T_f is the monopole formation time [which is an increasing function of M (Ref. 7)]. Now, M decreases with voltage owing to the dc bias condition,[7] so that the number of wells traversed by a monopole grows as the voltage increases (see Fig. 5). This means that the first term in Eq. (9) decreases with voltage and the second one increases with voltage (it becomes *less negative*). Thus there is a competition between these two mechanisms: the first tries to make the oscillation period decrease with voltage (therefore the oscillation frequency increases with voltage), while the second term has the opposite effect. Near the lowest voltage of an interval for which there are oscillations, $v_{mon} \approx v_M$, and the first term of Eq. (9) dominates. As

the voltage increases, the oscillation amplitude increases and v_{mon} decreases, so that the second term becomes more important. Of course whether the maximum of the frequency is reached immediately or not cannot be said from our rough argument. Still, the results of our simulations show conclusively that the oscillation frequency may reach a single maximum at voltage intervals where the current oscillates.

IV. CONCLUSIONS

Starting from a microscopic sequential-tunneling model of transport in weakly coupled SL, we have derived the field-dependent drift velocity for a doped 14/4 SL at temperatures ranging from 0 to 175 K. We found that the first plateau rapidly disappears as the temperature increases, and therefore we can set the diffusivity to zero in our DDD model to study the second plateau. Our numerical simulations show that stable solutions change from stationary field profiles with two coexisting electric-field domains at low temperature to recycling moving monopoles, giving rise to current self-oscillations at higher temperature. Voltage windows in the *I-V* diagram appear and widen as temperature increases. We observe as well an intrincate behavior of the oscillation frequency as a function of the dc voltage for different temperatures. These findings agree with and explain the experimental data reported by Wang *et al.*[17–19]

ACKNOWLEDGMENTS

This work was supported by the Spanish DGES through Grant Nos. PB98-0142-C04-01 and PB96-0875 and by European Union TMR Contract Nos. ERB FMBX-CT97-0157 and FMRX-CT98-0180.

APPENDIX: THE THEORETICAL EXPLANATIONS OF WANG *et al.*

The theoretical interpretation of experimental results in Refs. 17 and 18 is based upon a model proposed earlier by Wang and Niu (WN).[25] Their model is mathematically analogous to an earlier model of Laikhtman.[26] It consists of a system of rate equations

$$\frac{dq_i}{dt} = I_{i-1}(V_{i-1}) - I_i(V_i), \tag{A1}$$

$$V_i - V_{i-1} = kq_i, \tag{A2}$$

$$\sum_{i=0}^{N} V_i = V, \tag{A3}$$

with $i=1,\ldots,N$.[27] Equation (A1) is the charge continuity equation for the excess 2D electron charge density at the ith well, q_i (WN used the notation n_i instead of q_i). Here $I_i(V_i)$ is the tunneling current across the ith barrier, which depends only on the potential drop there, $V_i = \mu_i - \mu_{i+1}$, where μ_i is the chemical potential at the ith well. Equation (A2) is the Poisson equation with $k = 4\pi l^2/\varepsilon$, $l = d + w$. Last, Eq. (A3) is the dc voltage bias condition. The function $I_i(V_i)$ is in fact a piecewise linear N-shaped function common for all wells, $I(V_i)$; see Fig. 4 of Ref. 25.

Before commenting on this model, it is convenient to simplify it by eliminating the charge densities q_i. Notice that Eqs. (A1) and (A2) imply the usual Ampère's law

$$k^{-1}\frac{dV_i}{dt} + I_i(V_i) = \mathcal{I}, \tag{A4}$$

where $i=0,1,\ldots,N$ and $\mathcal{I}(t)$ is the total current.[26] Thus the model consists of $N+2$ equations, Eqs. (A3) and (A4) for $N+2$ unknowns, V_i, $i=0,1,\ldots,N$, and $\mathcal{I}$. The current $\mathcal{I}$ can be eliminated by adding all equations (A4) and using the fact that the bias (A3) is independent of time. The result is the following mean-field model:

$$\frac{dV_i}{dt} = -\frac{k}{N+1}\sum_{j=0}^{N}[I_i(V_i) - I_j(V_j)], \quad i=0,\ldots,N, \tag{A5}$$

$$\mathcal{I} = \frac{1}{N+1}\sum_{j=0}^{N} I_i(V_i). \tag{A6}$$

Equation (A5) is reminiscent of the problem of synchronization of coupled oscillators of zero frequency at zero temperature with the total current playing the role of order parameter.[28] The oscillators V_i try to achieve a stationary state such that $I_i(V_i) = \mathcal{I}$, given appropriate properties of the functions I_i (positive differential conductivity $dI_i/dV_i > 0$).[29]

1. Critique of the WN model and its analysis

The main physical objection to the WN model is that the sequential-tunneling current across a barrier, I_i, depends explicitly on the electron densities at adjacent wells, as well as on electrostatic potentials. This is made patent by microscopic derivations,[1,23] which are conspicuously absent in WN's paper. One unphysical consequence is that WN's results do not depend explicitly on well doping [except that $I_i(V_i)$ might change in some unspecified *ad hoc* form with doping]. However, experiments and theory show that stable static electric-field domains are formed at large doping, whereas self-sustained current oscillations appear for carrier densities below a critical value.[11] Similarly, doping at the injecting contact (ignored in the WN model) selects the type of charge density wave (monopoles or dipoles) responsible for current self-oscillations.[9]

WN's mathematical study of their model contains a linear stability analysis of a given unspecified stationary state and several unproven statements (some of which are even incorrect). Let us be specific. WN claim that all eigenvalues λ corresponding to inserting $E_i = A_i e^{\lambda t}$ in the linearized equations are real, which seems reasonable. However, later on, they claim that a time periodic solution (limit cycle) can appear via a Hopf bifurcation from a stationary state. This is an elementary error: a necessary condition of a Hopf bifurcation is that a pair of complex conjugate eigenvalues cross

the imaginary axis. The argument they use (illustrated in their Fig. 2) to ''prove'' the existence of a limit cycle rests on unproven assumptions and, anyway, is not valid in more than two dimensions. In fact, they claim that there exists a large enough region about an unstable stationary state which is invariant under the flow, because the potential difference between two adjacent wells cannot exceed the applied bias. But no one has proved that this model (not to be confounded with physical reality) posesses such a desirable property. Furthermore, if there is only one stationary state and it becomes unstable by changing a control parameter, it will typically do so by having one of its eigenvalues changing from negative to positive values. (Recall that all eigenvalues are real.) Then the bifurcating solution will typically (codimension 1) be stationary. Thus the situation of WN's Fig. 2 is unrealistic: inside the attractive region depicted, there should be another stationary (atracting) fixed point. Other more exotic possibilities are that the flow escapes to decidedly unphysical fixed points having some negative V_i or that it wanders chaotically between different unstable fixed points.

2. Anomalies

Wang *et al.*[18] gave an explanation for the fact that the self-oscillation frequency may increase with increasing bias while, at the same time, the mean current decreases. This allegedly anomalous behavior has been explained by means of the discrete drift model in Sec. III. On the other hand, the explanations of Wang *et al.* of the ''anomaly'' are based on the claim that Eq. (A4) with *constant* total current $\mathcal{I}$ can have a limit cycle. They also give an estimate of its frequency. These arguments are clearly erroneous. In fact, all equations in Eq. (A4) are uncoupled if $\mathcal{I}$ is a constant. Then Eq. (A4) is a one-dimensional autonomous dynamical system, which cannot have limit cycles among its solutions.

[1] A. Wacker, in *Theory and Transport Properties of Semiconductor Nanostructures*, edited by E. Schöll (Chapman and Hall, New York, 1998), Chap. 10.

[2] K.K. Choi, B.F. Levine, R.J. Malik, J. Walker, and C.G. Bethea, Phys. Rev. B **35**, 4172 (1987).

[3] H.T. Grahn, R.J. Haug, W. Müller, and K. Ploog, Phys. Rev. Lett. **67**, 1618 (1991).

[4] J. Kastrup, H.T. Grahn, K. Ploog, F. Prengel, A. Wacker, and E. Schöll, Appl. Phys. Lett. **65**, 1808 (1994).

[5] R. Aguado, G. Platero, M. Moscoso, and L.L. Bonilla, Phys. Rev. B **55**, R16 053 (1997).

[6] A.M. Tomlinson, A.M. Fox, and C.T. Foxon, Phys. Rev. B **61**, 12 647 (2000).

[7] J. Kastrup, R. Hey, K.H. Ploog, H.T. Grahn, L.L. Bonilla, M. Kindelan, M. Moscoso, A. Wacker, and J. Galán, Phys. Rev. B **55**, 2476 (1997).

[8] L.L. Bonilla, M. Kindelan, M. Moscoso, and S. Venakides, SIAM (Soc. Ind. Appl. Math.) J. Appl. Math. **57**, 1588 (1997).

[9] D. Sánchez, M. Moscoso, L.L. Bonilla, G. Platero, and R. Aguado, Phys. Rev. B **60**, 4489 (1999).

[10] O.M. Bulashenko and L.L. Bonilla, Phys. Rev. B **52**, 7849 (1995); Y. Zhang, J. Kastrup, R. Klann, K.H. Ploog, and H.T. Grahn, Phys. Rev. Lett. **77**, 3001 (1996).

[11] A. Wacker, M. Moscoso, M. Kindelan, and L.L. Bonilla, Phys. Rev. B **55**, 2466 (1997).

[12] M. Moscoso, J. Galán, and L.L. Bonilla, SIAM (Soc. Ind. Appl. Math.) J. Appl. Math. **60**, 2029 (2000).

[13] L.L. Bonilla, J. Galán, J.A. Cuesta, F.C. Martínez, and J. M. Molera, Phys. Rev. B **50**, 8644 (1994).

[14] N. Ohtani, N. Egami, H.T. Grahn, K.H. Ploog, and L.L. Bonilla, Phys. Rev. B **58**, R7528 (1998).

[15] N. Ohtani, N. Egami, H.T. Grahn, and K.H. Ploog, Phys. Rev. B **61**, R5097 (2000).

[16] B. Sun, J. Wang, W. Ge, Y. Wang, D. Jiang, H. Zu, H. Wang, Y. Deng, and S. Feng, Phys. Rev. B **60**, 8866 (1999).

[17] J.N. Wang, B.Q. Sun, X.R. Wang, Y. Wang, W. Ge, and H. Wang, Appl. Phys. Lett. **75**, 2620 (1999).

[18] X.R. Wang, J.N. Wang, B.Q. Sun, and D.S. Jiang, Phys. Rev. B **61**, 7261 (2000).

[19] C.Y. Li, B.Q. Sun, D.S. Jiang, and J.N. Wang, Semicond. Sci. Technol. **16**, 239 (2001).

[20] Y. Xu, A. Shakouri, and A. Yariv, J. Appl. Phys. **81**, 2033 (1997).

[21] H. Steuer, A. Wacker, E. Schöll, M. Ellmauer, E. Schomburg, and K.F. Renk, Appl. Phys. Lett. **76**, 2059 (2000).

[22] L.G. Mourokh, N.J.M. Horing, and A.Y. Smirnov, Appl. Phys. Lett. **78**, 1412 (2001).

[23] L.L. Bonilla, G. Platero, and D. Sánchez, Phys. Rev. B **62**, 2786 (2000).

[24] The tunneling current density ($\mathcal{J}$) through the ith barrier is a function of the densities at adjacent wells, n_i and n_{i+1}, and of the potential drops at barriers i and $i\pm1$; cf. Eq. (2) of Ref. 23. Over a wide temperature range, the tunneling current is *linear* in n_i and n_{i+1}. To calculate the drift velocity and electron diffusivity, we assume that the voltage drop $eF\mathcal{L}$ is the same within a SL period. Then $\mathcal{J}$ is a function of n_i, n_{i+1}, F, and temperature, and we use the formulas $v(F)=\mathcal{L}\mathcal{J}(N_D^w,N_D^w,F)/N_D^w$ and $D(F)=-\mathcal{L}^2\mathcal{J}(0,N_D^w,F)/N_D^w$.

[25] X.R. Wang and Q. Niu, Phys. Rev. B **59**, R12 755 (1999).

[26] B. Laikhtman, Phys. Rev. B **44**, 11 260 (1991).

[27] Reference 25 had a minus sign on the right-hand side of Eq. (A2), which was corrected in later papers.

[28] Y. Kuramoto, in *International Symposium of Mathematical Problems in Theoretical Physics*, edited by H. Araki, *Lecture Notes in Physics* Vol. 39 (Springer, New York, 1975), pp. 420–422; Y. Kuramoto, *Chemical Oscillations, Waves and Turbulence* (Springer, Berlin, 1984).

[29] In fact, $\mathcal{F}=[k/4(N+1)]\Sigma_{i=0}^{N}\Sigma_{j=0}^{N}[I_i(V_i)-I_j(V_j)]^2$ is a Lyapunov function for Eq. (A5) provided that all $I_i'(V_i)>0$: $\mathcal{F}\geqslant0$ and $d\mathcal{F}/dt=-\Sigma_{i=0}^{N}I_i'(V_i)(dV_i/dt)^2\leqslant0$ on the solutions of Eq. (A5).